Ultrasound Imaging: Principles and Applications in Rodent Research

Robert W. Coatney

Abstract

Ultrasound imaging utilizes the interaction of sound waves with living tissue to produce an image of the tissue or, in Doppler-based modes, determine the velocity of a moving tissue, primarily blood. These dynamic, real-time images can be analyzed to obtain quantitative structural and functional information from the target organ. This versatile, noninvasive diagnostic tool is widely used and accepted in human and veterinary medicine. Until recently, its application as a research tool was limited primarily to larger, nonrodent species. Due to advances in ultrasound imaging technology, commercially available ultrasound systems now have the spatial and temporal resolution to obtain accurate images of rat and mouse hearts, kidneys, and other target tissues, including tumor masses. As a result, ultrasound imaging is being used more frequently as a research tool to image rats and mice, and particularly to evaluate cardiac structure and function. The developing technology of ultrasound biomicroscopy has even greater spatial resolution and has been used to evaluate developing mouse embryos and guide site-specific injections into mouse embryos. Additional ultrasound imaging technologies, including contrast-enhanced imaging and intravascular ultrasound transducers adapted for transesophageal use, have been utilized in rats and mice. This paper provides an overview of basic ultrasound principles, equipment, and research applications. The use of noninvasive ultrasound imaging in research represents both a significant refinement as a potential replacement for more invasive techniques and a significant advancement in research techniques to study rats and mice.

Key Words: echocardiography; mice; rats; research; ultrasound

Robert W. Coatney, D.V.M., M.S., Ph.D., is Senior Staff Veterinarian in the Department of Laboratory Animal Sciences, GlaxoSmithKline, King of Prussia, Pennsylvania.

Introduction

Ultrasound imaging encompasses a wide range of imaging modes and techniques that utilize the interaction of sound waves with living tissues to produce an image of the tissues or, in the case of Doppler-based modes, determine a velocity of a moving tissue, primarily blood. Ultrasound imaging is a versatile, well-established, and widely used diagnostic tool in human and veterinary medicine. Its diagnostic applications include noninvasive imaging to characterize the structure, and in some applications the function, of target organs or masses, minimally invasive endocavity imaging with transesophageal and transrectal probes, and invasive imaging with intravascular probes. Before the early 1990s, research applications of ultrasound were limited primarily to larger animal species such as dogs, pigs, sheep, calves, and nonhuman primates. Advances in ultrasound imaging technology during the last decade have made it possible for commercially available medical ultrasound systems to obtain accurate and reliable images of rat hearts (Burrell et al. 1996; Cittadini et al. 1996; Forman et al. 1997; Litwin et al. 1994), mouse hearts (Scherrer-Crosbie et al. 1999a; Tanaka et al. 1996), and other target organs in rodents (Banic et al. 1993; Winters et al. 1997). Specialized ultrasound biomicroscopy systems have been developed to image fetal mouse hearts and organs (Aristizabal et al. 1998; Foster et al. 2000; Turnbull 1999; Turnbull et al. 1995; Srinivasan et al. 1998) and have been used to obtain high-resolution images of mouse tumors (Turnbull et al. 1996). Additionally, ultrasound imaging has been used to visualize and guide injections into target organs (Soots et al. 1998), including mouse embryos (Liu et al. 1998; Olsson et al. 1997), and to aid in the targeted delivery of compounds and viral constructs to specific target organs using contrast microbubbles (Mukherjee et al. 2000; Shotet et al. 2000). As a research tool, noninvasive ultrasound imaging represents not only a refinement in technique, but also a significant advancement in the ability to evaluate and quantitate target organ structure and function in rodent species.

This article provides an overview of basic ultrasound imaging principles, equipment, and common imaging for-

mats including brightness mode (B-mode[1]), motion mode (M-mode[1]), spectral Doppler, and color Doppler. Ultrasound biomicroscopy (UBM[1]), contrast-enhanced imaging, and transesophageal echocardiography (TEE[1]), three specialized ultrasound imaging techniques that have been used in rat and mouse research, are also reviewed. In light of the need to phenotype as well as obtain quantitative research information from genetically engineered mice, and the fact that the majority of animals used in research are rats and mice, the topics presented herein specifically focus on rat and mouse imaging. Examples of specific research applications are included in the overview of the imaging formats and specialized imaging techniques to help illustrate how ultrasound imaging is being used in research involving rats and mice.

Basic Ultrasound Imaging Principles, Equipment, and Imaging Formats

Ultrasound imaging principles, equipment, and imaging formats have been covered extensively in textbooks and numerous reviews. Furthermore, an encompassing overview of the subject is beyond the scope of this manuscript due to the variety and complexity of systems, techniques, and formats available, many of which are not useful for rodent imaging. Instead, the goal here is to provide a simplified overview of ultrasound imaging principles, equipment, and formats focusing on the considerations that are important when imaging rats and mice.

Basic Ultrasound Imaging Principles

Ultrasound refers to sound waves that are not detectable by the human ear with frequencies greater than 20,000 cycles/sec (Hz). Diagnostic ultrasound commonly uses frequencies between 2 and 15 MHz (10^6 cycles/sec). Intravascular transducers commonly use frequencies up to 30 MHz, and ultrasound biomicroscopy systems with transducers using frequencies up to 100 MHz have been reported (Foster et. al 2000; Turnbull et al. 1995). At these frequencies, sound waves are transmitted though soft tissue relative to the acoustic impedance of each tissue. The acoustic impedance of a particular tissue is the product of the transmission velocity of sound and the tissue density. The transmission velocity in most soft tissues and blood is nearly uniform at 1540 m/sec (Merritt 1998). Therefore, the acoustic impedance of most soft tissue is primarily a function of the tissue density. When two tissues with different densities are located next to each other, an acoustic impedance mismatch is created and sound waves are reflected by the mismatch.

The greater the acoustic mismatch or difference in tissue densities, the more sound waves are reflected and returned to the transducer. Areas with relatively large tissue density differences, and hence more reflected sound waves, are generally seen as brighter areas on the final image. As a result of these properties, ultrasound imaging is best suited for soft tissue imaging and is often limited by bone- and gas-filled structures. Sound is transmitted rapidly through bone tissue. Conversely, sound is poorly transmitted through air and air-filled structures. The large acoustic impedance mismatch that occurs at bone and gas interfaces with soft tissue causes the majority of sound waves to be reflected. This large reflection decreases sound wave penetration into deeper tissues and can cause imaging artifacts. Despite this limitation, specialized techniques have been developed to perform transcranial Doppler imaging of the cerebral vasculature in humans and dogs (Seidel et al. 2000).

Resolution, or the ability to distinguish two closely situated structures or events accurately, is an important concern for all imaging methodologies. However, resolution becomes even more important when imaging small targets such as rat and mouse organs. For example, the left ventricular (LV[1]) chamber diameter of a mouse heart is 2 to 3 mm and the LV posterior wall is approximately 0.6 mm thick at end diastole (Tanaka et al. 1996; Yang et al. 1999). In rodent ultrasound imaging, both spatial and temporal resolution must be considered. Spatial resolution is further divided into axial and lateral resolution.

Axial resolution is the ability to distinguish two separate but closely positioned structures situated parallel to the propagation axis of the ultrasound beam. Axial resolution is dependent on sound wave pulse length and frequency (wavelength). Two structures will be seen as separate structures only if the pulse length is shorter than the distance between the structures. If the pulse length is longer than the distance between the structures, only a single reflection will be detected and the image will show only one structure. Higher frequency sound waves have shorter pulse lengths and generally greater axial resolution.

Lateral resolution refers to the ability to distinguish two adjacent but separate structures oriented perpendicularly to the axis of the sound wave beam. Lateral resolution is dependent on beam width and sound wave frequency (Merritt 1998; Weyman 1994). Narrower beam width provides greater lateral resolution. Beam width can be minimized by focusing the sound waves as they are produced by the transducer. In most ultrasound systems, beam focusing is performed by curving the elements of the transducer or by electronically controlling the elements of the transducer. Lateral resolution is also influenced by the frequency of the sound wave, with higher frequencies generally improving resolution.

Because axial and lateral resolution improves with increasing frequency, higher frequency transducers are generally preferred for rat and mouse imaging. Rat hearts have been imaged using a variety of ultrasound systems with transducers operating at frequencies from 5 to 12 MHz (Behr et al. 2000; Haas et al. 1995; Isgaard et al. 1997; Litwin et al.

[1]Abbreviations used in this article: 2-D, two-dimensional; 3-D, three-dimensional; A waves, atrial contraction filling waves; B-mode, brightness mode; CPU, central processing unit; E waves, early filling waves; LV, left ventricular; M-mode, motion mode; TEE, transesophageal echocardiography; UBM, ultrasound biomicroscopy.

1994, 1995). Transducers that image at frequencies above 9 MHz are commonly used to image mouse hearts (Hoit et al. 1997; Scherrer-Crosbie et al. 1999a; Tanaka et al. 1996). Utilizing very high frequencies and narrow beam widths, UBM systems with 40- to 60-MHz transducers can have spatial resolution approaching 50 μm (Foster et al. 2000). One limitation of using higher frequencies is that as the frequency increases, sound wave penetration decreases. For example, a 5-MHz transducer will generally image to a depth of 12 to 15 cm, but a 10-MHz transducer may image to a depth of only 3 to 4 cm. Higher frequency UBM systems may penetrate only 1 to 2 cm. Hence, increasing axial and lateral resolution by increasing frequency limits the depth of penetration. Although this effect has a potential impact on transducer selection, it has minimal impact on imaging rats and mice because most of the target organs are generally within the penetration depth range (0.5-2 cm) of the higher frequency transducers. In larger species, this relation does influence transducer selection. A higher frequency transducer that could be used to image small nonhuman primates, such as marmosets, may not have the depth of penetration to image pigs or adult beagles.

Temporal resolution, or the ability to distinguish two events in time, is an important consideration when imaging rat and mouse hearts due to their fast heart rate (400-600 beats/min for the mouse, 300-500 beats/min for the rat). Temporal resolution is determined by the number of image frames that can be acquired per second, generally expressed in Hertz (Hz) or cycles per second. The importance of temporal resolution becomes evident when the number of images acquired per cardiac cycle is evaluated. For example, at a heart rate of 300 beats/min, an acquisition frame rate of 30 Hz (30 image frames/sec) would result in only six images/cardiac cycle. Moreover, each image frame would be acquired over 17% of the cardiac cycle, making the accurate determination of absolute end diastole and end systole difficult. In contrast, imaging a mouse heart beating at up to 600 beats/min with a frame rate of 150 Hz would acquire 15 frames over one cardiac cycle, greatly enhancing the temporal resolution. Several commercially available ultrasound systems can acquire at frame rates of 120 to 600 Hz. Although UBM offers greater spatial resolution, currently available systems have low imaging frame rates (5-10 Hz) and relatively poor temporal resolution for cardiac structures. The temporal resolution is not as critical when imaging target organs that are relatively nonmoving, such as the kidney.

Equipment

The basic components of all ultrasound systems include a central processing unit (CPU[1]) or computer, a transducer (or several different transducers depending on the applications), a monitor, and a system to store the images. The CPU controls and processes the majority of the functions of the ultrasound system. It is responsible for the input to the other components such as the transducer and monitor. It also receives and analyzes electronic input from the transducer ultimately to construct the image. The CPU provides the tools for analyzing and obtaining quantitative measurements from the images. It can also serve as a temporary storage system for images. All ultrasound systems have a CPU; however only the most recent generation ultrasound systems have the computing capabilities and speed needed for high-resolution imaging at the high frame rates that are essential for imaging mouse hearts. These systems also have fully digital image processing capabilities. One advantage of the latest generation of ultrasound systems is that they can be upgraded easily by installing software as technology advances, rather than requiring purchase of an entirely new system.

The transducer is essentially the "working arm" of an ultrasound system. It produces the sound waves and receives reflected sound waves. Transducers contain piezoelectric crystals that vibrate when exposed to small electrical currents, thereby producing the sound waves. These crystals also produce small electrical currents when they are deformed by reflected sound waves. Sound waves produced by these crystals are focused into a beam and transmitted through the soft tissues of the body and target organ. The transducer then pauses for a short period of time to receive the reflected sound waves. Each tissue through which the sound waves pass has a slightly different acoustic impedance, which is relative to the density of the tissue. At the interface of two different tissues, an acoustic impedance mismatch occurs, and some sound waves are reflected. These reflected sound waves interact with the piezoelectric crystals in the transducer to produce a small current. These electrical signals are processed by the CPU, and the image is constructed and displayed on a monitor.

A wide variety of transducers are available for each commercial ultrasound system. Transducers are most commonly "hand held," but they can be located on the tip of a catheter for intravascular applications or on a stationary arm for UBM. The application of these transducers varies with the working frequency range and the crystal element design. Multielement linear and phased array transducers are most commonly used in imaging rodents. In certain imaging applications, more than one transducer may be needed to capitalize on the strengths and capabilities of each transducer. Understanding the capabilities and limitation of each transducer is critical in obtaining high-quality accurate images. In general, it is advisable to use the highest frequency transducer that will penetrate to the depth of the target structure (Merritt 1998).

Image storage systems can vary greatly between ultrasound systems. Prior to ultrasound systems with fully digital image processing capabilites, videotape and printed copies of the images were the common storage media. State-of-the-art systems store a limited number of images digitally; however, the images still must be transferred to another computer system, such as a workstation, or stored on magneto-optical diskettes. The process of digital storage and archiving of images allows for easier retrieval and analysis of images and

does not subject the images to the loss of resolution that occurs when they are stored on videotape. With digital image storage, image analysis can be performed using the ultrasound system or a compatible workstation.

Numerous ultrasound systems, each with several transducer and software options, are readily available from several manufacturers. However, only a few systems have been used to image rats and mice. Commercially available ultrasound systems and transducer frequencies that have been used to image rats and mice and have been cited in published manuscripts are listed in Table 1. In general, the latest generation of ultrasound systems with higher frequency transducers (higher spatial resolution) and high-imaging frame rates are those most capable of imaging rats and mice.

Imaging Formats

B-Mode or Two-dimensional Imaging

The most common imaging format for general use is B-mode, in which the image is constructed and displayed on the monitor as a gray-scaled, two-dimensional (2-D[1]) image or cross-section of the target organ that is moving in real time (Figure 1). Hence, it is also commonly referred to as 2-D or real-time ultrasound. The resulting "real time" image incorporates information about the target organ structure as well as motion and function. 2-D imaging has been used to determine target organ size and appearance and, if the acquisition frame rate is sufficient to provide accurate temporal resolution, to determine changes in target organ size over time and assess function. 2-D imaging has been used to evaluate LV structure and function in rats (Bing et al. 1995) and mice (Pollick et al. 1995; Scherrer-Crosbie et al. 1999a). In these studies, LV chamber dimensions were determined at end diastole and systole and were used to calculate cardiac function parameters such as stroke volume, cardiac output, ejection fraction, and fractional shortening. Reconstruction of three-dimensional (3-D[1]) volumes using multiple 2-D images has been described for numerous species, including the mouse (Scherrer-Crosbie et al. 1999a). This 3-D volumetric reconstruction of the mouse LV was validated by correlating the calculated stroke volume and cardiac output with values obtained using an implanted aortic flow probe. LV mass has

Table 1 Commercially available ultrasound systems and transducers used for rat and mouse imaging

Species	Ultrasound System, Manufacturer	Transducer	References (see text)
Mouse	Sequoia, Acuson Corp., Mountain View, CA	15L8 (13 MHz)	Scherrer-Crosbie et al. 1999a Scherrer-Crosbie et al. 1999b Takeishi et al. 2000 Youn et al. 1999
Mouse	Sonos 5500, Agilent Technologies (Hewlett-Packard, Palo Alto, CA)	12 MHz	Gao et al. 2000 Mor-Avi et al. 1999
Mouse	HDI5000cv, ATL Ultrasound, Inc., Bothell, WA	L12-5 (12 MHz)	Esposito et al. 2000
Mouse	HDI3000, ATL Ultrasound Inc., Bothell, WA	10 MHz	Patten et al. 1998
Mouse	Apogee CX, ATL Ultrasound Inc., Bothell, WA	9.0 MHz	Tanaka et al. 1996
Mouse	128XP/10, Acuson Corp., Mountain View, CA	7.0 MHz	Manning et al. 1994 Gardin et al. 1995
Rat	VingMed System Five GE Medical Systems, Milwaukee, WI	10 MHz	Sjaastad et al. 2000
Rat	HDI5000cv, ATL Ultrasound Inc., Bothell, WA,	L12-5 (12 MHz)	Behr et al. 2000
Rat	128XP/10, Acuson Corp.,Mountain View, CA	7.0 MHz	Burrell et al. 1996 Mulder et al. 1998
Rat	Sonos 2500 Hewlett Packard (Agilent Technologies, Palo Alto, CA)	7.5 MHz	Isgaard et al. 1997
Rat	Sonos 1500 Hewlett Packard (Agilent Technologies, Palo Alto, CA)	7.5 MHz	Cittadini et al. 1996 Schwarz et al. 1998a,b
Rat	Sonos 1000 Hewlett Packard (Agilent Technologies, Palo Alto, CA)	7.5 MHz	Bing et al. 1995
Rat	Model 77020A Hewlett Packard (Agilent Technologies, Palo Alto, CA)	5 MHz	Haas et al. 1995
Rat	Interspec XL-3 ATL Interspec (ATL Ultrasound Inc., Bothell, WA)	7.5 MHz	Pawlush et al. 1993

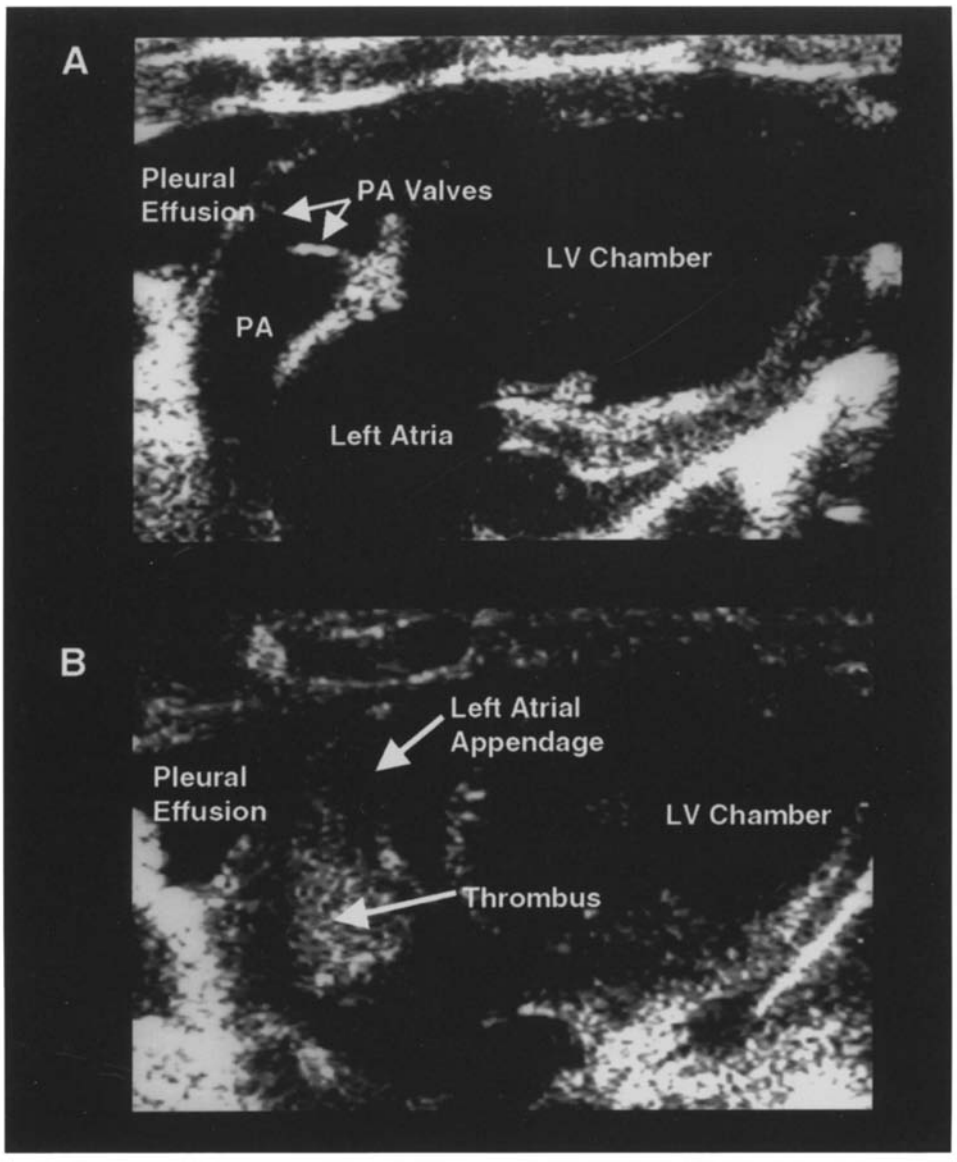

Figure 1 Two-dimensional (2-D) long axis cardiac images from a spontaneously hypertensive heart failure rat (SHHF/MccGmi-*fa*^{cp}). (A) End diastolic 2-D image revealing a dilated left atria and greatly dilated left ventricle (LV). Pleural effusion is evident between the cardiac structures and the sternum. The pulmonary artery (PA) and pulmonary valves are also seen in the image. (B) 2-D image obtained to the left of image A revealing a greatly dilated left atrial appendage with a large left atrial thrombus. The LV and pleural effusion are also evident. (Images obtained using HDI5000cv, L12-5 transducer, ATL Ultrasound, Bothell, Washington.)

also been calculated using 2-D images and has been validated for mice (Youn et al. 1999).

Although the most common application of 2-D imaging in rats and mice has been in evaluating cardiac structure and function, it has also been used to evaluate other target organs. 2-D imaging has been used to evaluate renal structure in an autosomal recessive polycystic kidney disease model in mice (Winters et al. 1997). It also has been used for ultrasound-guided injection of recombinant adenovirus in rabbits (Weig et al. 2000) and ultrasound-guided renal biopsy in rats (Soots et al. 1998). In addition, 2-D imaging is used as a "guidance" system for other imaging formats, such as M-mode and spectral and color flow Doppler, and enables the operator/sonographer to optimize positioning in these formats.

M-Mode

M-mode is commonly used in imaging the heart or echocardiography. An M-mode echocardiogram is obtained with a single ultrasound beam transmitted through the heart or target tissue, and the resulting image is displayed over time.

An M-mode echocardiogram has depth on the Y axis and time on the X axis. It can be conceptualized as an "ice-pick" view of the heart displayed in motion across time (Figure 2). In M-mode imaging, the ultrasound beam width is minimized, and acquisition frame rates generally increase, resulting in an increase in spatial and temporal resolution compared with 2-D imaging. Information that can be obtained from an M-mode echocardiogram includes LV wall thickness and chamber dimensions at various time points throughout the cardiac cycle, but most commonly at end systole and diastole (Figure 3). M-mode echocardiograms have been used to assess LV structure and function in rats (Burrell et al. 1996; Cittadini et al. 1996; Forman et al. 1997; Litwin et al. 1994, 1995; Pawlush et al. 1993) and mice (Fentzke et al. 1997; Gardin et al. 1995; Manning et al. 1993; Pollick et al. 1995; Tanaka et al. 1996). End diastolic and end systolic volumes can be calculated from the measured LV chamber dimensions and used to quantitate LV function using stroke volume, cardiac output, and percent ejection fraction. These calculations are based on geometric assumptions regarding the shape of the ventricle. If the ventricle changes shape between evaluations or the geometric assumption is incorrect for the shape of the ventricle, the calculated values can be inaccurate. The use of M-mode echocardiography-derived measurements to quantitate LV mass has been validated in the rat (de Simone et al. 1990) and mouse (Manning et al. 1994).

Both 2-D and M-mode have been used to evaluate cardiac structure and function in genetically engineered mouse models (Christensen et al. 1997; Esposito et al. 2000; Lim et al. 2000; Mor-Avi et al. 1999; Takeishi et al. 2000; Vatner et al. 2000), naturally occurring and induced models of cardiac hypertrophy and heart failure in rats and mice (Gao et al.

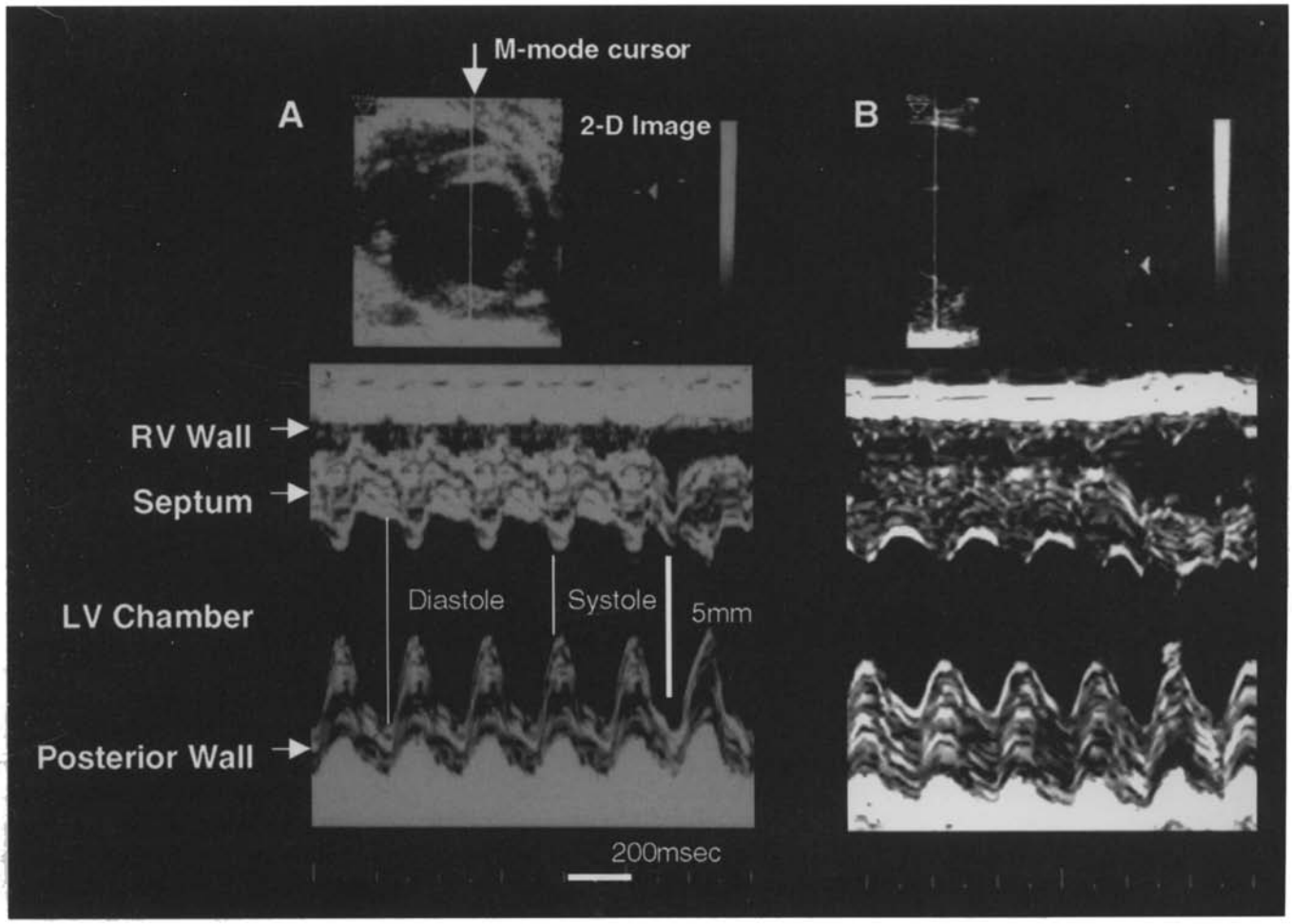

Figure 2 Motion mode (M-mode) images from a spontaneously hypertensive-stroke prone (SHR-SP) rat. Both A and B are two-dimensional guided M-mode images obtained from the midpapillary muscle region of the left ventricle (LV). Distance (mm) from the transducer is on the Y axis; time (msec) is on the X axis. The M-mode images show the right ventricular (RV) wall, septum, LV chamber, and LV posterior wall throughout diastole and systole. (A) Baseline M-mode image. (B) M-mode obtained from the same rat that had consumed a high-fat (24.5% in food) and high-salt (1% in water) diet for 12 wk. Note the thicker septum and LV posterior wall during diastole and the decreased end diastole LV chamber diameter. (Images obtained using HDI5000cv, L12-5 transducer, ATL Ultrasound, Bothell, Washington.)

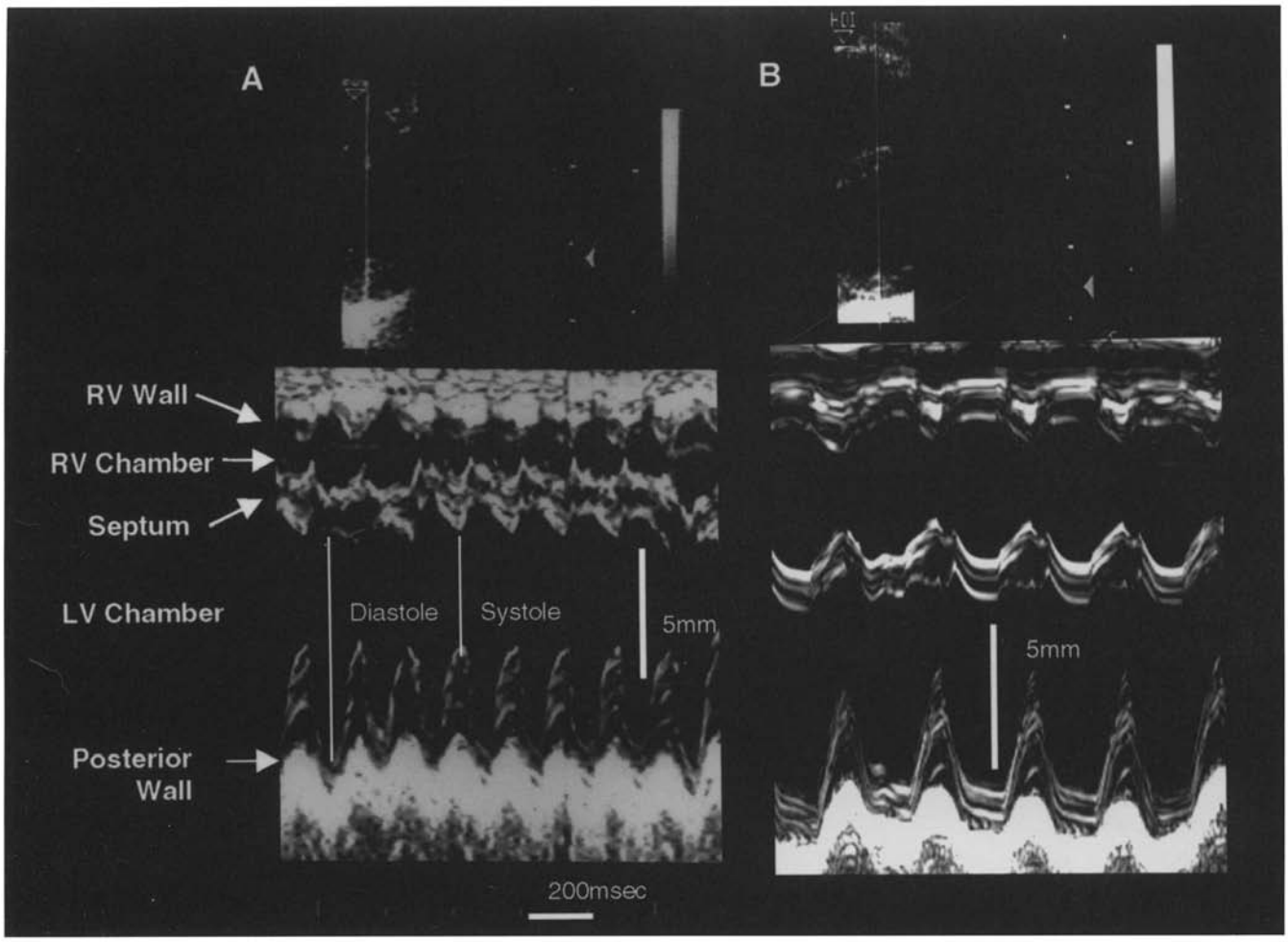

Figure 3 Motion mode (M-mode) images from a Wistar-Kyoto rat. Both A and B were obtained from the midpapillary region of the left ventricle (LV) using two-dimensional (2-D) guidance. (A) Baseline M-mode image. (B) M-mode image from the same rat after 6 days of volume overload induced by creating an aortocaval shunt. Note the increased thickness of the right ventricular (RV) wall and the marked increase in RV and LV end diastolic chamber diameters. (Images obtained using HDI5000cv, L12-5 transducer, ATL Ultrasound, Bothell, Washington.)

2000; Haas et al. 1995; Inoko et al. 1994; Litwin et al. 1994; Patten et al. 1998; Pawlush et al. 1993; Schwarz et al. 1998a; Tanaka et al. 1996), and pharmacological effects of various agents in some of these models (Behr et al. 2000; Isgaard et al. 1997; Lim et al. 2000; Litwin et al. 1995; Mulder et al. 1998). Both formats acquire and display images of 3-D structures in a 2-D format. As a result, the LV volumes and mass are calculated using measurements of structures from two or more 2-D images or a single M-mode echocardiogram. These mathematical calculations are based on assumptions regarding the geometry of the left ventricle.

The approach described above has been well documented for echocardiography (Vuille and Weyman 1994) and is applicable until the shape of the target organ changes to the degree that the geometrical assumptions are no longer valid. M-mode-derived volume and mass calculations are particularly susceptible to this type of error because they are based on a single measurement from a single point through the ventricle and do not include a ventricular length measurement. Volume and mass calculations utilizing multiple measurements from multiple 2-D images to mathematically reconstruct ventricular volumes and mass are less vulnerable to the influences and errors associated with the geometric assumptions. This approach has been used to perform 3-D mathematical reconstruction of the LV volumes and mass for mice (Scherrer-Crosbie et al. 1999a; Youn et al. 1999). This approach can be more accurate than calculating ventricular volumes from single 2-D or M-mode image, but it can be influenced by inaccurate registration of adjacent 2-D images. One approach for solving these problems is to acquire volumetric 3-D images (Arbeille et al. 2000; Shiota et al. 1999). 3-D image acquisition systems have been developed; however, at the time of this writing, none have the spatial or temporal resolution to be used in rats and mice.

Doppler Imaging

Spectral Doppler and color flow Doppler imaging modes utilize the Doppler shift principle to determine blood flow velocity and direction. With respect to ultrasound imaging, the Doppler effect is the apparent shift in sound wave frequency that occurs when a sound wave is reflected by a moving target—primarily blood cells. If the blood cells are flowing toward the transducer, the frequency of the reflected waves is higher than the original transmitted waves. If the blood is flowing away from the transducer, the frequency of the reflected waves is lower than that of the original transmitted waves. This difference in transmitted and reflected wave frequency is the "Doppler shift" (Merritt 1998). The greater the Doppler shift, the greater the velocity of the flow blood. The Doppler shift is affected by the alignment of the ultrasound beam and the flowing blood. As this alignment diverges from parallel, the detected Doppler shift is attenuated. As a result of this relation, it is important to orient the ultrasound beam as parallel as possible to the direction of flow or movement. In most situations, completely parallel alignment is not possible, so it has been recommended that the alignment be no greater than 20 to 30° from parallel. Even this angle of alignment is often difficult to obtain, especially when imaging peripheral vessels, and mouse and rat hearts. Angle correction is used in some situations. The angle between the flow axis and the ultrasound beam (incident angle) is used in the Doppler calculation to correct for the attenuation of the Doppler shift (Merritt 1998).

Spectral Doppler displays the velocity within a specific region within a vessel over time (Merritt 1998). The result is a velocity profile (Figure 4). Spectral Doppler can be either

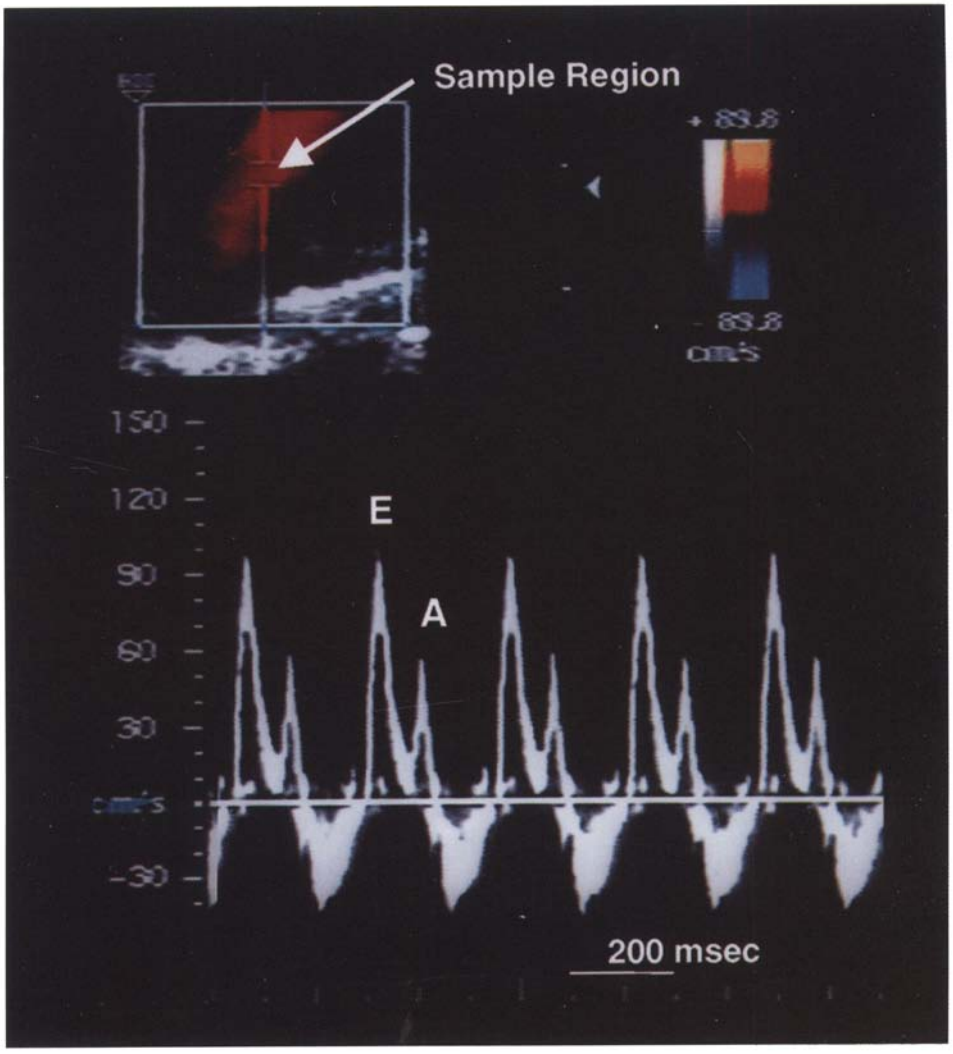

Figure 4 Mitral inflow velocity profile obtained from a spontaneously hypertensive-stroke prone (SHR-SP) rat using pulsed wave spectral Doppler. The velocity profile is obtained from blood flowing within the sample region shown on the two-dimensional image. The velocity (cm/sec, Y axis) of the blood flowing through the sample region is shown over time (msec, x axis). The early (E) velocity peak that occurs during left ventricular relaxation and the atrial (A) velocity peak that occurs during atrial contraction are evident. (Images obtained using HDI5000cv, L12-5 transducer, ATL Ultrasound, Bothell, Washington.)

pulsed wave or continuous wave. In pulsed wave Doppler, a single transducer produces and transmits the sound waves and then receives the reflected sound waves, whereas in continuous wave Doppler, one transducer produces and transmits the sound waves and a second transducer detects the reflected sound waves. One advantage of pulsed wave Doppler is that it allows the determination of the velocity profile from a precise location (range resolution) using a 2-D image for guidance and then obtaining the velocity from a specific area or "sample volume." However, the maximum flow velocity that can be accurately detected by pulsed wave Doppler is limited. In contrast, continuous wave Doppler can detect higher flow velocities than pulsed wave Doppler but is not capable of range resolution.

The flow velocity profile obtained from both pulsed and continuous wave Doppler can be analyzed to provide various parameters that are used to evaluate cardiac or peripheral vasculature functions (Feigenbaum 1994). Hartley and colleagues (1995) used a 20-MHz pulsed wave Doppler system to obtain blood flow velocities from the ascending aorta of mice and to evaluate cardiac function using peak systolic velocity and acceleration times. Similar techniques have been used to demonstrate cardiac function differences in hyperthyroid mice (Taffet et al. 1996) and hemodynamic alterations in apolipoprotein E knockout mice (Hartley et al. 2000). One limitation of this system is that it lacks 2-D imaging capabilities for accurate range resolution to guide placement of the Doppler sample volume. This limitation requires aiming the transducer toward the target flow area or vessel and moving it until the proper waveform is identified.

Transmitral flow velocity profiles have been used to evaluate diastolic function in humans (Choong 1994). Similarly, transmitral flow velocity profiles have been obtained from rats (Forman et al. 1997; Litwin et al. 1994) and mice (Pollick et al. 1995; Taffet et al. 1996). The resulting early filling waves (E waves[1]) and atrial contraction filling waves (A waves[1]) were measured and the E:A ratio used to estimate LV relaxation. Although this approach to evaluating LV relaxation has been reported for rats and mice, it is complicated by the evidence that at normal resting heart rates for rats and mice, the E and A waves are commonly fused. Sjaastad and coworkers (2000) report that transmitral E and A wave separation is heart rate dependent in the rat, and that the waves fuse at heart rates faster than 320 beats/min.

Blood flow or stroke volume can also be calculated as the product of the cross-sectional area (cm^2) of the vessel or outflow tract and the velocity-time integral (cm/sec) derived from the flow velocity profile. This calculation has been used to estimate cardiac output and stroke volume in rats (Litwin et al. 1994) and mice (Hartley et al. 1995). One potential advantage of using spectral Doppler flow velocity to calculate stroke volume and cardiac output is that it does not rely on mathematical calculations based on geometric assumptions about the shape of the ventricle. For this reason, it is relatively independent of the LV geometry, which may change during the course of an experiment or be different in different animal models. However, the difficulty in obtaining consistent, near-parallel alignment of the sound waves with the aortic outflow often limits the application of this technique.

Color flow Doppler represents a color-encoded map of flow velocity and direction superimposed on a 2-D image (Figure 5). One color from a preset color flow map is assigned to a flow velocity and direction. These images display the velocity and direction of the blood flow in the specific target structure in real time. Diagnostically, color flow maps have been used to evaluate valvular competency and valvular regurgitation in the heart and to evaluate turbulence in peripheral vessel flow at sites of stenosis or vessel damage. Research applications of color flow maps have been limited, especially in rodents. Mitral regurgitation in rats (Forman et al. 1997) and aortic regurgitation in the mouse (Pollick et al. 1995) have been detected using color flow Doppler. Color flow Doppler may be useful in phenotyping genetically altered mice.

In addition to the four basic imaging formats and modes described above, ultrasound offers numerous specialized imaging formats and techniques that are used routinely in diagnostic imaging. Many of these formats have not been applied or shown to be useful in imaging rats and mice. However, three techniques—UBM, contrast-enhanced imaging, and TEE—have been used successfully in imaging rats and mice. Potential sources for UBM and TEE equipment and contrast agents are listed in Table 2.

Ultrasound Biomicroscopy

Ultrasound biomicroscopy utilizes ultrasound imaging to visualize tissue at microscopic resolution. It has also been termed ultrasound backscatter microscopy and high- or very high-frequency ultrasound imaging. Ultrasound biomicroscopy technology and applications have been reviewed (Foster et al. 2000). These systems commonly use single-element mechanical transducers that operate at frequencies of 30 to 100 MHz. UBM is capable of acquiring images using 2-D B-mode, pulsed and continuous wave Doppler, and color flow Doppler. Although most of these systems are custom made for specific research applications, systems are also available commercially. Ultrasound biomicroscopy transducers with frequencies of 30 to 100 MHz have been reported to have axial resolution ranging from 60 to 19 μm and lateral resolution ranging from 250 to 60 μm (Foster et al. 2000). Doppler imaging resolution is also enhanced using high-frequency sound waves. Goertz and colleagues (2000) have shown that UBM color flow Doppler is capable of detecting flow in arterioles between 15 and 20 μm in diameter in the mouse ear. Despite the greatly improved spatial resolution, these systems have limited temporal resolution and depth penetration. With imaging frame rates of 5 to 10 Hz and depth of penetration often limited to 2 to 10 mm, cardiac imaging applications in adult rats and mice are restricted.

Clinical applications for UBM include ocular and dermal imaging (Foster et al. 2000; Pavlin and Foster 1995). High-resolution UBM images of the cornea and anterior chamber

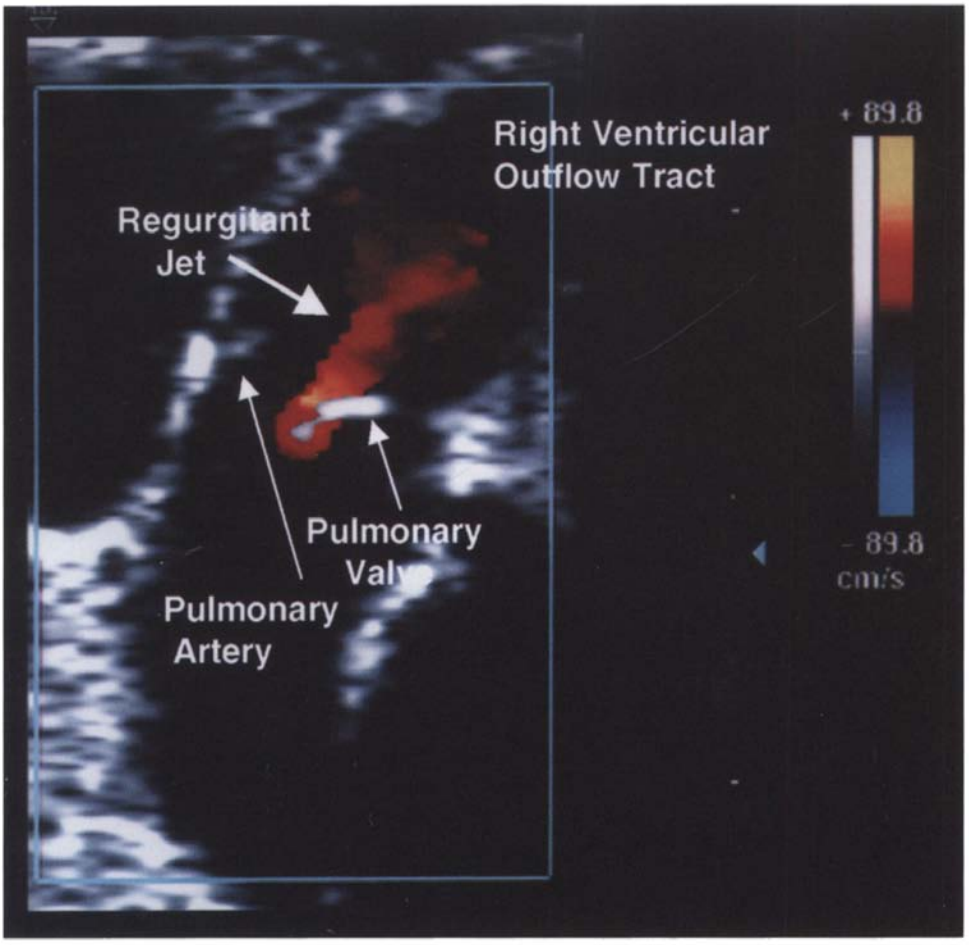

Figure 5 Color Doppler image of the pulmonary artery of a spontaneously hypertensive heart failure (SHHF/MccGmi-*fa*^{cp}) rat. The color bar indicates the colors assigned to velocities in the directions toward and away from the transducer (top of image). The large area of flow across the pulmonary valves toward the transducer and into the right ventricular outflow tract indicates a large regurgitant flow across the pulmonary valves due to valvular insufficiency. (Images obtained using HDI5000cv, L12-5 transducer, ATL Ultrasound, Bothell, Washington.)

structures have been used to evaluate corneal disease and trauma, anterior segment tumors, and glaucoma (Foster et al. 2000; Silverman et al. 1995). In the research setting, color flow maps of the vasculature of the rabbit eye, including the arterial circulation of the anterior ciliary body, ciliary processes, and iris, have been produced using UBM (Kruse et al. 1998). In this study, flow velocities as low as 0.2 mm/sec were detected in vessels as small as 40 μm in diameter. Ocular UBM has also been used to evaluate hereditary glaucoma in inbred DBA/2J mice (John et al. 1998).

Dermal UBM has been used to determine skin thickness and wound healing (Hoffman et al. 1993), assess dermal blood flow (Christopher et al. 1997), and define tumor margins (Harland et al. 1993). The progression of implantable murine melanoma tumors in C57/BL/6 mice has been studied using similar techniques (Turnbull et al. 1996). Considerable effort is being made to advance this technology to evaluate tumor angiogenesis, produce 3-D flow maps, and quantitate blood flow across tumor areas (Foster et al. 2000).

Fatkin and colleagues (1999) used 2-D UBM imaging to evaluate cardiac structure in neonatal transgenic mice that developed a progressive dilated cardiomyopathy. Srinivasan and coworkers (1998) used UBM to image living mouse embryos in utero and follow the development of cardiac structures as well as changes in blood flow velocities in the heart and umbilical artery. This technique might be useful in determining embryological development in genetically manipulated mice as well as during exposure to novel compounds. UBM has also been used to guide the injection of cells and retroviruses into specific locations of developing mouse embryos (Gaiano et al. 1999; Liu et al. 1998; Olsson et al. 1997).

Contrast-enhanced Ultrasound Imaging

Microbubbles filled with inert gas are used as ultrasound contrast agents. Because sound waves are highly reflected from gas-filled structures, these microbubbles increase the amount of sound waves returning to the transducer and increase the signal-to-noise ratio. Contrast agents can be used to enhance 2-D as well as spectral and color Doppler imag-

Table 2 Potential sources for UBM, contrast imaging, and intravascular ultrasound catheters for TEE[a]

Product	Application	Source / Manufacturer	References (see text)
20 MHz pulsed wave Doppler system	Pulsed wave Doppler for cardiac and peripheral vascular evaluation	Indus Instruments Houston, TX	Hartley et al. 1995, 2000 Taffet et al. 1996
ClearView Ultra, ClearView Cross Catheters	Intravascular ultrasound system for TEE in mice and rats	Boston Scientific Scimed, Inc. Maple Grove, MN	
In-Vision IVUS System	Intravascular ultrasound system for TEE in mice and rats	JOMED (Endosonics) Rancho Cordova, CA	
CVIS	Intravascular ultrasound system for TEE in mice and rats	Cadiovascular Imaging Systems Sunnyvale, CA	Lu et al. 1997
Model 840	UBM	Humphreys Instruments San Leandro, CA	Fatkin et al. 1999
VS40 Ultrasound Biomicroscope	UBM	VisualSonics Toronto, Canada	
P40 Ultrasound Biomicroscope	Ocular imaging, UBM	Paradigm Medical Industries Salt Lake City, UT	
Definity	Contrast agent	DuPont Pharmaceuticals Billerica, MA	Scherrer-Crosbie et al. 1999b
Optison	Contrast agent	Mallinkrodt, Inc. St. Louis, MO	

[a]TEE, transesophageal echocardiography; UBM, ultrasound biomicroscopy.

ing. In the most simple applications, these contrast microbubbles have been used to improve visualization of target organs and cardiac chambers. Mor-Avi and colleagues (1999) describe the use of contrast imaging to improve visualization of endocardial borders of the left ventricle in mice. Contrast-enhanced imaging has also been used to evaluate perfusion of tissues, commonly myocardium and tumors. Scherrer-Crosbie and coworkers (1999b) report the use of contrast echocardiography to evaluate myocardial perfusion after coronary artery ligation in mice. In this study, perfusion deficits were imaged in all mice after coronary artery ligation, and the deficit size determined by contrast imaging was significantly correlated with the nonperfused area determined by Evans blue staining.

Contrast agents also react to the sound waves they encounter. High-energy sound waves can rupture the microbubbles. This property of ultrasound-mediated destruction of microbubbles has been used for targeted delivery of compounds to specific organs or locations. It has also been used to enhance the transfection of myocardial cells with adenovirus-linked transgenes. Shotet and colleagues (2000) report that targeted ultrasound-mediated destruction of microbubbles coated with recombinant adenovirus containing a beta-galactosidase and constitutive promoter increased myocardial transfection and beta-galactosidase activity compared with nondisrupted microbubbles and viral construct infusion.

TEE

TEE is an established technology in human diagnostic imaging. Due to the close apposition of the esophagus, heart, and great vessels, TEE provides an ideal window for cardiovascular imaging because there is little attenuation of the sound waves by lung and other tissues. All of the commercially available TEE transducer systems have diameters too large for use in rodents. A full-function (2-D, M-mode, and spectral and color Doppler) 10 French (3.2-mm) diameter intracardiac catheter system has recently become available and adapted for transesophageal echocardiography in rabbits (Bruce et al. 1999). Despite this success in transesophageal echocardiography in rabbits weighing 400 to 3400 g, the use of this catheter system in smaller rats and mice has not been demonstrated.

To take advantage of the transesophageal window and improve imaging of the right ventricle and great vessels in rats and mice, TEE has been performed using high-frequency, intravascular transducers (Kupferwasser et al. 1998; Scherrer-Crosbie et al. 1998; Schwarz et al. 1998b). These intravascular ultrasound transducers operate at higher frequencies (20-30 MHz) than most commercially available transthoracic transducers and are located at the tip of a catheter. In mice, TEE using a 3.5 French (1.1-mm) diameter 30-MHz intravascular transducer has been used to determine

right ventricular diastolic and systolic volumes, assess stroke volume and cardiac output, measure right ventricular wall thickness (Scherrer-Crosbie et al. 1998), and demonstrate right ventricular hypertrophy in response to hypoxia. This technique has also been used to demonstrate that mice congenitally deficient in endothelial nitric oxide synthase exhibit greater right ventricular hypertrophy in response to hypoxia-induced pulmonary hypertension (Steudel et al. 1998). A similar intravascular transducer was used to evaluate vegetative lesions on the aortic valves of rats serially (Kupferwasser et al. 1998). In this study, the vegetative lesions measured using TEE correlated well with the size of lesions measured postmortem. TEE using intravascular transducers has also been used to evaluate LV structure in rats. Lu and colleagues (1997) reported good correlation between LV structure and mass determined by TEE using an 8 French 20-MHz intravascular transducer and transthoracic 2-D echocardiography. In contrast, Schwarz and coworkers (1998b) reported that TEE using a 6 French 20-MHz intravascular transducer provided only semiquantitative images because the apical portion of the left ventricle could not be visualized. These authors further concluded that noninvasive transthoracic echocardiography provided better quality and more quantifiable images. The cause of the disagreement regarding the utility of TEE to evaluate LV structures can only be speculated upon but may be due to differences in the transducers and the depth of penetration capabilities. One limitation of using intravascular catheter-tipped transducers for TEE is that these transducers commonly have lower imaging frame rates and therefore lower temporal resolution than is commonly obtained using transthoracic echocardiography. Despite the apparent disagreement about the utility of TEE to evaluate LV structures in the rat, TEE provides better images of the rat aorta and atria.

Advantages and Disadvantages of Ultrasound Imaging

As with any technology used in research, ultrasound imaging has advantages and disadvantages. A significant advantage of ultrasound imaging over other research techniques is that it is noninvasive. Its advantages over other imaging techniques relate to its capability, versatility, portability, safety, and economic feasibility. Commercially available ultrasound imaging systems are capable of spatial resolution approaching that of magnetic resonance microscopy as a result of advances in transducer and computing technology. These same advances have also increased temporal resolution such that accurate imaging of mouse hearts is feasible. Ultrasound biomicroscopy further increases the spatial resolution of these noninvasive imaging systems and presents great potential to adapt and apply this technology to many research applications, especially in mice.

Ultrasound imaging captures dynamic, real-time images that can be analyzed to obtain quantitative structural and functional information from many different target organs. This real-time format gives ultrasound imaging particular advantage in imaging moving targets such as the heart and blood. Its utility in rat and mice echocardiography is evident from the numerous publications cited. Its multiple imaging modes and formats add to its versatility as well as its capability and adaptability. Other than possibly magnetic resonance microscopy, no other technique can provide the same structural and functional information that can be obtained by ultrasound imaging. Imaging a mouse heart, after proper training and sufficient practice, is easier than implanting aortic flow probes or sonomicrometer crystals.

Because ultrasound imaging is noninvasive and a well-accepted human diagnostic tool, it can be used on most species utilized in research, from mouse to humans, including developing embryos. This versatility allows it to serve as a bridge technology in which the procedures and techniques used in human medicine or human clinical trails can be essentially the same as those used in animal studies. In addition, many of the techniques used for echocardiography in rats and mice are based on those currently used in human echocardiography. Within the frequencies used for imaging, ultrasound is accepted as safe and harmless to tissues and living organisms. Furthermore, the contrast agents employed do not require ionizing radiation and have been shown to be safe for use in human medicine. Commercial ultrasound systems are compact and portable. The current generation of ultrasound systems can be upgraded easily by installing new software, rather than replacing the entire system. Compared with most other imaging technologies, ultrasound imaging systems are far less expensive and do not require specialized facilities or renovations.

Ultrasound imaging also has limitations and disadvantages as a research tool. One particular limitation is that it requires the knowledge and expertise of a well-trained and skilled operator/sonographer (hereafter referred to as operator) to obtain accurate, repeatable, high-quality images. This requirement is due in part to the fact that the resolution, anatomical image accuracy, and image quality are influenced and can be controlled by the person acquiring the image. The operator must have a good understanding of ultrasound technology, the capabilities and limits of the ultrasound system and transducers, and a thorough knowledge and understanding of the anatomy and function of the target organ. Furthermore, because ultrasound imaging is operator dependent, there can be small differences in the images obtained by two different operators. The impact of this limitation can be addressed by utilizing a single operator to image all animals on a given study. The person analyzing the image can also influence the accuracy of the quantitative data. Therefore, the person analyzing the data must also be well skilled and analyze the data consistently. Despite these concerns and limitations, low inter- and intraobserver variability has been reported for M-mode echocardiography in the rat (Litwin et al. 1994) and M-mode and 2-D echocardiography in the mouse (Scherrer-Crosbie et al. 1999a; Tanaka et al. 1996). Moreover, numerous publications indicate that ultrasound imaging has been used successfully to determine differences

in cardiac structure and function in rats and mice despite these concerns.

In humans and many larger species, ultrasound imaging is routinely performed on conscious, nonanesthetized subjects. In contrast, the majority of studies published to date using ultrasound imaging in rats and mice have been performed imaging anesthetized subjects. The fact that most anesthetic agents can affect cardiac function could be considered a limitation. At the time of this writing, there is one publication demonstrating the feasibility of performing ultrasound imaging in conscious mice (Yang et al. 1999). However, it is necessary to weigh the effect of restraint-induced stress against that of an anesthetic agent in deciding whether to attempt imaging in conscious rodents.

The remaining limitations of ultrasound imaging relate to the characteristics of the imaging modality. As previously mentioned, ultrasound imaging is limited by bone- and gas-filled structures, therefore ultrasound is not routinely capable of brain and spinal cord imaging. Abdominal ultrasound can also be affected by gas-filled intestinal segments. Not all ultrasound systems have the temporal resolution to accurately image mouse hearts, so care must be taken to monitor and determine the imaging frame rate of a given application and system. Ultrasound imaging also has less spatial resolution at deep tissues due to the frequency (wavelength)-dependent inverse relation between resolution and depth of penetration. Although this is not currently a significant limitation when imaging rats and mice using commercially available systems, it might limit the utility of ultrasound biomicroscopy in imaging deeper structures in these species.

Although ultrasound imaging is quite capable of obtaining images that can be quantified to provide structural and functional information, it is far less capable of obtaining metabolic, chemical, and binding interaction information compared with other imaging techniques. Due to the fact that ultrasound imaging relies on an externally generated signal rather than a tissue-specific chemical signal, as in the case of magnetic resonance imaging phosphorous spectroscopy, it does not provide information about the chemical and metabolic status of the tissue it is imaging. Although there is interest in developing ultrasound contrast agents with specific surface ligands for binding location and quantification, positron emission tomography is currently more capable of these types of studies.

Ultrasound Imaging as Refinement and Advancement in Technology

The application of noninvasive ultrasound imaging in research, and particularly the imaging of rats and mice, represents both a significant refinement and an advance in research techniques. As a refinement in research technique, ultrasound imaging can replace more invasive techniques that cause pain and distress. For example, transthoracic echocardiography has been used to evaluate LV morphology and function. In this application, it can be used to determine cardiac output and stroke volume and thereby replace the use of surgically implanted aortic flow probes or sonomicrometer crystals. This use not only reduces animal pain and distress, but it also obviates a postoperative healing and recovery period as well as possible implant-related complications. Furthermore, transthoracic echocardiography has been validated for the determination of LV mass. Before the application of ultrasound to determine LV mass in rats and mice, the most common method of determining LV mass was euthanasia and weighing of the harvested LV. Because ultrasound imaging is noninvasive, LV mass can be followed serially in the same animal, thus reducing the number of animals required for a study as well as increasing statistical power, with each animal serving as its own control. This capability to determine structural and functional progression of target organ or tumor disease processes, and response to a therapy noninvasively, is indeed a powerful advantage of ultrasound imaging.

Ultrasound imaging also represents a significant advancement in research techniques for rats and mice. For evaluating rat and mouse heart structure and function, there is essentially no other single technique, invasive or noninvasive, that can provide the same detailed information as quickly and accurately as properly performed ultrasound imaging.

Summary

Ultrasound imaging is a versatile, dynamic multiformat imaging technology that has many current and potential applications in research and, in particular, research using rats and mice. Additionally, noninvasive ultrasound imaging represents a significant refinement as well as an advance in the ability to obtain quantitative structural and functional information from many different target organs. Many commercially available ultrasound systems now have spatial and temporal resolution to image many target organs in rats and mice accurately. In particular, the use of ultrasound imaging in cardiovascular research using rats and mice has increased steadily since the mid-1990s, and it is becoming an essential tool in phenotyping and studying genetically engineered mice. The focus on developing high-frequency, high-resolution transducers in ultrasound biomicroscopy will likely further improve ultrasound imaging capabilities, and particularly in work with mice. The rapidly advancing field of diagnostic ultrasound imaging holds the promise of new imaging formats and technologies that will further improve the imaging of small research animals.

References

Arbeille P, Eder V, Casset D, Quillet L, Hudelo C, Herault S. 2000. Real-time 3-D ultrasound acquisition and display for cardiac volume and ejection fraction evaluation. Ultrasound Med Biol 26:210-208.

Aristizabal O, Christopher DA, Foster FS, Turnbull DH. 1998. 40-MHz echocardiography scanner for cardiovascular assessment of mouse embryos. Ultrasound Med Biol 24:1407-1417.

Banic A, Geiser D, Wanner M, Larsen SE. 1993. Doppler duplex for the

evaluation of the degree of stenosis in carotid arteries in the rat. J Reconstruct Microsurg 9:237-243.

Behr TM, Wang X, Aiyar N, Coatney RW, Li X, Koster P, Angermann CE, Ohlstein E, Feuerstein GZ, Winaver J. 2000. Monocyte chemoattractant protein-1 is upregulated in rats with volume-overload congestive heart failure. Circulation 102:1315-1322.

Bing OH, Brooks WW, Robinson KG, Slawsky MT, Hayes JA, Litwin SE, Sen S, Conrad CH. 1995. The spontaneously hypertensive rat as a model of the transition from compensated left ventricular hypertrophy to failure. J Mol Cell Cardiol 27:383-396.

Bruce CJ, Packer DL, O'Leary PW, Seward JB. 1999. Feasibility study: Transesophageal echocardiography with a 10F (3.2 mm), multifrequency (5.5- to 10-MHz) ultrasound catheter in a small rabbit model. J Am Soc Echocardiogr 12:596-600.

Burrell LM, Chan R, Phillips PA, Calafiore P, Tonkin AM, Johnston CI. 1996. Validation of an echocardiographic assessment of cardiac function following moderate size myocardial infarction in the rat. Clin Exp Pharm Physiol 23:570-572.

Choong CY. 1994. Left ventricular V: Diastolic function—Its principles and evaluation. In: Weyman AE, ed. Principles and Practices of Echocardiography. Philadelphia: Lea and Febiger. p 721-780.

Christensen G, Wang Y, Chien KR. 1997. Physiological assessment of complex cardiac phenotypes in genetically engineered mice. Am J Physiol 272(Pt2):H2113-H2124.

Christopher DA, Burns PN, Starkoski BG, Foster FS. 1997. A high frequency pulsed-wave Doppler ultrasound system for the detection and imaging of blood flow in the microcirculation. Ultrasound Med Biol 7:997-1015.

Cittadini A, Stromer H, Katz SE, Clark R, Moses AC, Morgan JP, Douglas PS. 1996. Differential cardiac effects of growth hormone and insulin-like growth factor-1 in the rat: A combined in vivo and in vitro evaluation. Circulation 93:800-809.

de Simone G, Wallerson DC, Volpe M, Devereux RB. 1990. Echocardiographic measurement of left ventricular mass and volume in normotensive and hypertensive rats: Necropsy validation. Am J Hypertens 3:688-696.

Esposito G, Santana LF, Dilly K, Cruz JD, Mao L, Lederer WJ, Rockman HA. 2000. Cellular and functional defects in a mouse model of heart failure. Am J Physiol Heart Circ Physiol 279:H3103 - H3112.

Fatkin D, Christe ME, Aristizabal O, McConnell BK, Srinivasan S, Schoen FJ, Seidman CE, Turnbull DH, Siedman JG. 1999. Neonatal cardiomyopathy in mice homozygous for the Arg403Gln mutation in the alpha myosin heavy chain gene. J Clin Invest 103:147-153.

Feigenbaum H. 1994. Echocardiography. 5th ed. Baltimore: Williams & Wilkins.

Fentzke RC, Korcarz CE, Shroff SG, Lin H, Sandelski J, Leiden JM, Lang RM. 1997. Evaluation of ventricular and arterial hemodynamics in anesthetized closed-chest mice. J Am Soc Echocardiograph 10:915-925.

Forman DE, Cittadini A, Azhar G, Douglas PS, Wei JY. 1997. Cardiac morphology and function in senescent rats: Gender-related differences. J Am Coll Cardiol 30:1872-1877.

Foster FS, Pavlin CJ, Harasiewicz KA, Christopher DA, Turnbull DH. 2000. Advances in ultrasound biomicroscopy. Ultrasound Med Biol 26:1-27.

Gaiano N, Kohtz JD, Turnbull DH, Fishell G. 1999. A method for rapid gain-of-function studies in the mouse embryonic nervous system. Nat Neurosci 2:812-819.

Gao XM, Dart AM, Dewar E, Jennings G, Du XJ. 2000. Serial echocardiographic assessment of left ventricular dimensions and function after myocardial infarction in mice. Cardiovasc Res 45:330-338.

Gardin JM, Siri FM, Kitsis RN, Edwards JG, Leinwand LA. 1995. Echocardiographic assessment of left ventricular mass and systolic function in mice. Circ Res 76:907-914.

Goertz DE, Christopher DA, Yu JL, Kerbel RS, Burns PN, Foster FS. 2000. High frequency color flow imaging of the microcirculation. Ultrasound Med Biol 1:63-71.

Haas GJ, McCune SA, Brown DM, Cody RJ. 1995. Echocardiographic characterization of left ventricular adaptation in a genetically determined heart failure rat model. Am Heart J 130:806-811.

Harland C, Bamber J, Gusterson B, Mortimer P. 1993. High-frequency, high resolution B-scan ultrasound assessment of skin tumours. Br J Dermatol 128:525-232.

Hartley CJ, Michael LH, Entman ML. 1995. Noninvasive measurement of ascending aortic blood velocity in mice. Am J Physiol 268(Pt 2):H499-505.

Hartley CJ, Reddy AK, Madala S, Martin-McNulty B, Vergona R, Sullivan ME, Halks-Miller M, Taffet GE, Michael LH, Entman ML, Wang YX. 2000. Hemodynamic changes in apolipoprotein E knockout mice. Am J Physiol Heart Circ Physiol 279:H2326 -2334.

Hoffman K, Winkler K, el-Gammal S, Altmeyer P. 1993. A wound healing model with sonographic monitoring. Clin Exp Dermatol 18:217-225.

Hoit BD, Khan ZU, Pawloski-Dahm CM, Walsh RA. 1997. In vivo determination of ventricular wall stress-shortening relationship in normal mice. Am J Physiol 272(Pt2):H1047-H1052.

Inoko M, Kihara Y, Morii I, Fujiwara H, Sasayama S. 1994. Transition from compensatory to dilated, failing left ventricles in Dahl salt-sensitive rats. Am J Physiol 267(Pt2):H2471-H2482.

Isgaard J, Kujacic V, Jennische E, Holmang A, Sun XY, Hedner T, Hjalmarson A, Bengtsson BA. 1997. Growth hormone improves cardiac function in rats with experimental myocardial infarction. Eur J Clin Invest 27:517-525.

John SW, Smith RS, Savinova OV, Hawes NL, Chang B, Turnbull D, Davisson M, Roderick TH, Heckenlively JR. 1998. Essential iris atrophy, pigment dispersion, and glaucoma in DBA/2J mice. Invest Ophthalmol Vis Sci 39:951-962.

Kruse D, Fornaris J, Silverman R, Coleman D, Ferrara KW. 1998. A swept-scanning mode for estimation of blood velocities in the microvasculature. IEEE Trans Ultrason Ferroelec Freq Control 45:1437-1440.

Kupferwasser I, Darius H, Buerke M, Rupprecht HJ, Mohr-Kahaly S, Meyer J. 1998. Transesophageal ultrasonographic imaging in rat hearts: Visualization of aortic vegetations in non-bacterial thrombotic endocarditis. J Am Soc Echocardiogr 11:201-205.

Lim HW, De Windt LJ, Mante J, Kimball TR, Witt SA, Sussman MA, Molkentin JD. 2000. Reversal of cardiac hypertrophy in transgenic disease models by calcineurin inhibition. J Mol Cell Cardiol 32:697-709.

Litwin SE, Katz SE, Morgan JP, Douglas PS. 1994. Serial echocardiographic assessment of left ventricular geometry and function after large myocardial infarction in the rat. Circ 89:345-354.

Litwin SE, Katz SE, Weinberg EO, Lorell BH, Aurigemma GP, Douglas PS. 1995. Serial echocardiographic-Doppler assessment of left ventricular geometry and function in rats with pressure-overload hypertrophy. Chronic angiotensin-converting enzyme inhibition attenuates the transition to heart failure. Circulation 91:2645-2654.

Liu A, Joyner AL, Turnbull DH. 1998. Alteration of limb and brain patterning in early mouse embryos by ultrasound-guided injection of Shh-expressing cells. Mech Dev 75:107-115.

Lu L, Ko E, Schwartz GG, Chou TM. 1997. Transesophageal echocardiography in rats using an intravascular ultrasound catheter. Am J Physiol 273(Pt2):H2078-2082.

Manning WJ, Wei JY, Katz SE, Douglas PS, Gwathmey JK. 1993. Echocardiographically detected myocardial infarction in the mouse. Lab Animal Sci 43:583-585.

Manning WJ, Wei JY, Katz SE, Litwin SE, Douglas PS. 1994. In vivo assessment of LV mass in mice using high-frequency cardiac ultrasound: Necropsy validation. Am J Physiol 266:H1672-H1675.

Merritt CR. 1998. Physics of ultrasound. In: Rumack CM, Wilson SR, Charboneau, eds. Diagnostic Ultrasound. St. Louis: Mosby. p 3-35.

Mor-Avi V, Korcarz C, Fentzke RC, Lin H, Leiden JM, Lang RM. 1999. Quantitative evaluation of left ventricular function in a transgenic mouse model of dilated cardiomyopathy with 2-dimensional contrast echocardiography. J Am Soc Echocardiogr 12:209-214.

Mukherjee D, Wong J, Griffin B, Ellis SG, Porter T, Sen S, Thomas JD. 2000. Ten-fold augmentation of endothelial uptake of vascular endothelial growth factor with ultrasound after systemic administration. J Am Soc Echocardiogr 35:1678-1686.

Mulder P, Richard V, Bouchart F, Derumeaux G, Munter K, Thuillez C. 1998. Selective ETA receptor blockade prevents left ventricular

remodeling and deterioration of cardiac function in experimental heart failure. Cardiovasc Res 39:600-603.

Olsson M, Campbell K, Turnbull DH. 1997. Specification of mouse telecephalon and mid-brain progenitors following heteropic ultrasound-guided embryonic transplantation. Neuron 19:761-772.

Patten RD, Aronovitz MJ, Deras-Mejia L, Pandian NG, Hanak GG, Smith JJ, Mendelsohn ME, Konstam MA. 1998. Ventricular remodeling in a mouse model of myocardial infarction. Am J Physiol 274(Pt2):H1818-H1820.

Pavlin CJ, Foster FS. 1995. Ultrasound Biomicroscopy of the Eye. New York: Springer-Verlag.

Pawlush DG, Moore RL, Musch TI, Davidson WR. 1993. Echocardiographic evaluation of size, function and mass of normal and hypertrophied rat ventricles. J Appl Physiol 74:2598-2605.

Pollick C, Hale SL, Kloner RA. 1995. Echocardiographic and cardiac Doppler assessment of mice. J Am Soc Echocardiogr 8(Pt1):602-610.

Scherrer-Crosbie M, Steudel W, Hunziker PR, Foster GP, Garrido L, Liel-Cohen N, Zapol WM, Picard MH. 1998. Determination of right ventricular structure and function in normoxic and hypoxic mice: A transesophageal echocardiography study. Circulation 98:1015-1021.

Scherrer-Crosbie M, Steudel W, Hunziker PR, Liel-Cohen N, Ullrich R, Zapol WM, Picard MH. 1999a. Three-dimensional echocardiographic assessment of left ventricular wall motion abnormalities in mouse myocardial infarction. J Am Soc Echocardiogr 12:834-840.

Scherrer-Crosbie M, Steudel W, Ullrich R, Hunziker PR, Liel-Cohen N, Newell J, Zaroff J, Picard MH. 1999b. Echocardiographic determination of risk area size in a murine model of myocardial infarction. Am J Physiol 277(Pt2):H986-992.

Schwarz ER, Pollick C, Dow J, Patterson M, Birnbaum Y, Kloner RA. 1998a. A small animal model of non-ischemic cardiomyopathy and its evaluation by transthoracic echocardiography. Cardiovasc Res 39:216-223.

Schwarz ER, Pollick C, Meehan WP, Kloner RA. 1998b. Evaluation of cardiac structure and function in small experimental animals: Transthoracic, transesophageal, and intravascular echocardiography to assess contractile function in rat heart. Basic Res Cardiol 93:477-486.

Seidel G, Algermissen C, Christoph A, Katzer T, Kaps M. 2000. Visualization of brain perfusion with harmonic gray scale and power Doppler technology: An animal pilot study. Stroke 31:1728-1734.

Shiota T, McCarthy PM, White RD, Qin JX, Greenberg NL, Flamm SD, Wong J, Thomas JD. 1999. Initial clinical experience of real-time three-dimensional echocardiography in patients with ischemic and idiopathic dilated cardiomyopathy. Am J Cardiol 84:1068-1073.

Shotet RV, Chen S, Zhou YT, Wang Z, Meidell RS, Unger RH, Grayburn PA. 2000. Echocardiographic destruction of albumin microbubbles directs gene delivery to the myocardium. Circulation 101:2554-2556.

Silverman RH, Rondeau MJ, Lizzi Fl, Coleman DJ. 1995. Three-dimensional high-frequency ultrasonic parameter imagining of anterior segment pathology. Ophthalmology 102:837-843.

Sjaastad I, Sejersted OM, Hebekk A, Bjornerheim R. 2000. Echocardiographic criteria for detection of postinfarction congestive heart failure in rats. J Appl Physiol 89:1445-1454.

Soots A, Lautenschlager I, Krogerus L, Saarinen O, Ahonen J. 1998. An experimental model of chronic renal allograft rejection in the rat using triple drug immunosuppression. Transplantation 65:42-46.

Srinivasan S, Baldwin HS, Aristizabal O, Kwee L, Labow M, Artman M, Turnbull DH. 1998. Noninvasive, in utero imaging of mouse embryonic heart development with 40 MHz echocardiography. Circulation 98:912-918.

Steudel W, Scherrer-Crosbie M, Bloch KD, Weimann J, Huang PL, Jones RC, Picard MH, Zapol WM. 1998. Sustained pulmonary hypertension and right ventricular hypertrophy after chronic hypoxia in mice with congenital deficiency of nitric oxide synthase 3. J Clin Invest 191:2468-2477.

Taffet GE, Hartley CJ, Wen X, Pham T, Micheal LH, Entman ML. 1996. Noninvasive indexes of cardiac systolic and diastolic function in hyperthyroid and senescent mouse. Am J Physiol 270(Pt2):H2204-H2209.

Takeishi Y, Ping P, Bolli R, Kirkpatrick DL, Hoit BD, Walsh RA. 2000. Transgenic overexpression of constitutively active protein kinase C epsilon causes concentric cardiac hypertrophy. Circ Res 86:1218-1223.

Tanaka N, Dalton N, Mao L, Rockman HA, Peterson KL, Gottshall KR, Hunter JJ, Chien KR, Ross J. 1996. Transthoracic echocardiography in models of cardiac disease in the mouse. Circulation 94:1109-1117.

Turnbull DH. 1999. In utero ultrasound backscatter microscopy of early stage mouse embryos. Comput Med Imaging Graphics 23:25-31.

Turnbull DH, Bloomfield TS, Baldwin HS, Foster FS, Joyner AL. 1995. Ultrasound backscatter microscope analysis of early mouse embryonic brain development. Proc Natl Acad Sci U S A 92:2239-2243.

Turnbull DH, Ramsay JA, Shivji GS, Bloomfield TS, From L, Sauder DN, Foster FS. 1996. Ultrasound backscatter microscope analysis of mouse melanoma progression. Ultrasound Med Biol 22:845-853.

Vatner DE, Yang GP, Geng YJ, Asai K, Yun JS, Wagner TE, Ishikawa Y, Bishop SP, Homey CJ, Vatner SF. 2000. Determinants of the cardiomyopathic phenotype in chimeric mice overexpressing Gs alpha. Circ Res 86:802-806.

Vuille C, Weyman AE. 1994. Left ventricle I: Assessment of size and function. In: Weyman AE, ed. Principles and Practices of Echocardiography. 2nd ed. Philadelphia: Lea and Febiger. p 575-624.

Weig HJ, Laugwitz KL, Moretti A, Kronsbein K, Stadele C, Bruning S, Seyfarth M, Brill T, Schomig A, Ungerer M. 2000. Enhanced contractility after gene transfer of V2 vasopressin receptors in vivo by ultrasound guided injection or transcoronary delivery. Circulation 101:1578-1585.

Weyman AE, ed. 1994. Principles and Practices of Echocardiography. 2nd ed. Philadelphia: Lea and Febiger.

Winters WD, McDonald RA, Krauter LD. 1997. The detection of murine autosomal recessive polycystic kidney disease using real time ultrasound. Ped Nephrol 11:337-338.

Yang XP, Liu YH, Rhaleb NE, Kurihara N, Kim HE, Carretero OA. 1999. Echocardiographic assessment of cardiac function in conscious and anesthetized mice. Am J Physiol 277(Pt2):H1967-H1974.

Youn HJ, Rokosk G, Lester SJ, Simpson P, Schiller NB, Foster E. 1999. Two-dimensional echocardiography with a 15 MHz transducer is a promising alternative for in vivo measurement of left ventricular mass in mice. J Am Soc Echocardiographr 12:70-75.